Gridless Sparse Recovery-based Wind Speed Estimation for Wind-shear Detection using Airborne Phased Array Radar

Zhiming ZHENG [1,2], Jizhou LAI [1], Qieqie ZHANG [1], Jingru GUO [1]
[1] College of Automation Engineering, Nanjing University of Aeronautics and Astronautics, Nanjing, China
[2] COMAC Shanghai Aircraft Design and Research Institute, Shanghai, China

zhengzhiming@comac.cc

Submitted March 17, 2024 / Accepted June 17, 2024 / Online first August 19, 2024

Abstract. *The accuracy of wind speed estimation is an important factor affecting wind-shear detection in airborne weather radar. Aiming at the problem that dictionary mismatch in the sparse recovery-based wind speed estimation leads to the performance degradation, this paper proposes a wind speed estimation method based on atomic norm minimization for airborne array weather radar. The method first constructs joint sparse recovery measurements by compensating multiple array element data with wind-shear orientation information, and then the wind speed is estimated on continuous parameter domain using atomic norm minimization with multiple compensated measurements. Simulation experiments demonstrate that the proposed method can effectively improve the accuracy of wind speed estimation under dictionary mismatch, and the performance is better than that of the existing sparse recovery-based method of wind speed estimation with the pre-set discretized dictionary.*

Keywords

Wind speed estimation, wind-shear detection, airborne phased array weather radar

1. Introduction

Airborne weather radar is a type of radar used to provide an indication to pilots of the intensity of convective weather [1]. Weather can be a hazard to aircraft in many ways. Wind-shear is one of the most dangerous conditions, which is the change in speed and direction of wind suddenly over a relatively short distance or time period, it is also called wind gradient [2]. Low altitude wind-shear (LAWS) is recognized as a major hazard during takeoff and landing of an aircraft. When the wind-shear occurs below 600 m during takeoff or landing, the pilot has little time to react correctly to maintain safe flight [3], as shown in Fig. 1. According to the record, in the United States between 1964 and 1985, there were 26 major civil transport aircraft accidents caused 626 fatalities for which wind-shear was a direct cause or a contributing factor [4]. One of the most notable accident was a Delta Air Lines crash in 1985, wind-shear caused the aircraft to lose lift and crash short of the runway, killing 137 passengers.

Radar technology developments have allowed more accurate wind-shear detection. Through the detection of the frequency shift of the microwave pulses, airborne radar is now capable of detecting wind-shear and changes in wind speed close to the ground [5]. All commercial jet aircraft must have an airborne forward-looking weather radar with a solution for detecting wind-shear since 1993, according to FAA regulations (RTCA DO-220A) [6].

One of the major problems associated with wind-shear detection using an airborne weather radar is the presence' of ground clutter. When the airborne weather radar detects wind-shear for aircraft landing, the radar is in a down-looking mode, the received signal of the wind-shear is mixed with the signal of ground clutter. In order to detect the wind-shear effectively, the ground clutter must be suppressed before wind-shear detection [7]. Recently, phased array radar (PAR) has demonstrated the high-resolution estimation of accurate Doppler speed when compared to mechanically scanning radar. The space-time adaptive processing (STAP) is an effective method for clutter suppression in airborne phased array radar systems [8], and it has been used for ground clutter suppression before wind-shear detection in airborne weather radar [9], [10].

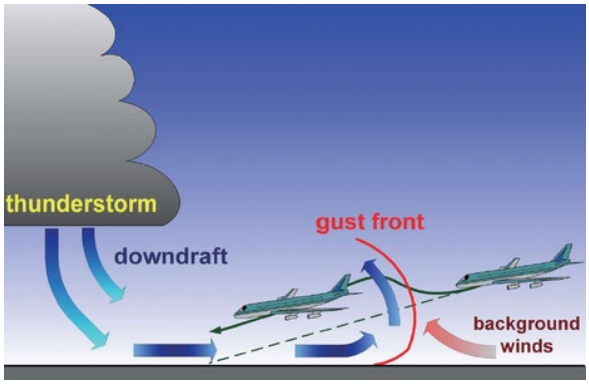

Fig. 1. Wind-shear encounter during approach.

DOI: 10.13164/re.2024.0494

The F-factor is a quantitative measurement of the effect of the wind-shear to either increase or decrease the performance of the aircraft [11]. The results were evaluated to determine the capability of the radar to detect and alert of hazardous wind-shear. The F-factor is calculated by the wind speed, since, wind speed estimation is the most important step of wind-shear detection. Some methods of wind speed estimation have been proposed for wind-shear detection. Baxa proposed the pulse pair processing method (PPP) [12], and it is used in Collins WXR-700 airborne weather. Briit proposed the fast Fourier transform-based (FFT) wind speed estimator [13]. In the case of adequate measurements, the PPP and FFT methods can get a good performance. However, sufficient measurements are hardly obtained in practical applications. The performance of wind speed estimation degrades significantly in the case of insufficient measurements. In order to improve the performance of wind speed estimation and reduce the number of required samples, the sparse recovery-based wind speed estimator jointly with STAP was proposed for airborne phased array weather radar [14], termed as on-grid CS method. Sparse recovery approaches have gained great attention due to their ability to provide innovative solutions to the problems of signal estimation, where the signal is sparse on some basis vectors [15]. In the above-mentioned sparse recovery-based wind speed estimator, the wind speed parameter domain has been uniformly discretized into small grid points, and the wind speed has been assumed to be located exactly in the pre-discretized grid points on the parameter domain. The set of parameter vectors of all grid points is called the wind speed dictionary. However, wind speed is continuously distributed on the parameter domain, and the wind speed estimates are not even located on the grids, which is known as the off-grid effect [16]. The accuracy of sparse recovery-based wind speed estimator relies on the discretized wind speed dictionary, and the performance degrades significantly due to the off-grid effect. Recently, continuous compressive sensing (CCS) has been proposed for super-resolution sparse recovery, i.e., atomic ℓ_0 norm [17]. For the low-rank property of the covariance matrix, the atomic ℓ_1 norm, i.e., atomic norm, was proposed as a computationally feasible alternative to the atomic ℓ_0 norm, to reconstruct the atoms in the continuous-valued frequency domain by utilizing Vandermonde decomposition [16]. Inspired by the super-resolution property of the atomic norm minimization, this paper extends the atomic norm minimization to the wind speed estimation, and a gridless super-resolution sparse recovery wind speed estimator based on the atomic norm minimization with multiple measurements is proposed. In the proposed method, first, the multiple measurements for sparse recovery are constructed by compensating multiple array elements with the wind orientation information. Then, the wind speed is estimated in the continuous-value parameter domain using the atomic norm minimization, and the off-grid problem caused by the discretized dictionary is fully avoided. Due to the super-resolution property of the atomic norm minimization, the proposed method can achieve more accurate estimations of the wind speed than the existing approaches. Simulations are conducted to demonstrate the wind speed estimation performance of the proposed method, and the results show that the proposed method can achieve significant improvement compare to the presently available methods.

There are two major contributions in the proposed method:

- The wind speed is estimated on continuous parameter domain using atomic norm minimization, then the off-grid effect in sparse recovery-based wind speed estimator is avoided.
- Joint sparse recovery measurements by compensating multiple array element data with wind-shear orientation are constructed to enhance the performance of sparse recovery.

The rest of the paper is organized as follows. Section 2 introduces the signal model of an airborne phased array weather radar. Section 3 reviews the sparse recovery-based wind speed estimate approaches and then explains the off-grid effect. Section 4 presents the proposed method. Section 5 presents the simulation results to demonstrate the performance of the proposed method. Section 6 provides the conclusion.

Notations used in this paper are as follows. $\boldsymbol{A}^{\mathrm{T}}$ and $\boldsymbol{A}^{\mathrm{H}}$ denote the matrix transpose and conjugate transpose of $\boldsymbol{A}$, respectively; $\otimes$ denotes the Kronecker product; $\mathbb{R}$ and $\mathbb{C}$ denote the sets of real and complex numbers, respectively; the upper and lower cases boldface letters denote matrices and vectors, respectively; rank(·) denotes the rank, and tr(·) denotes the trace.

2. Signal Model

This paper considers a uniformly linear array (ULA) forward-looking airborne array weather radar, which consists of M antenna elements having a spacing of half of wavelength ($d = \lambda/2$) and where N pulses are received during the coherent processing interval (CPI) at a constant pulse repetition frequency (PRF) f_{r}. The geometry of the radar is shown in Fig. 2, the platform has an altitude H and moves with a constant velocity v_{p} along the x axis. The received signal of radar in the lth ($l = 1,2,\ldots,L$) range bin can be expressed as:

$$\boldsymbol{x}^{(l)} = \boldsymbol{x}_{\mathrm{s}}^{(l)} + \boldsymbol{x}_{\mathrm{c}}^{(l)} + \boldsymbol{x}_{\mathrm{n}}^{(l)} \tag{1}$$

where $\boldsymbol{x}$ is an NM-dimensional measurement vector, and it is called the space-time snapshot; $\boldsymbol{x}_{\mathrm{s}}$ is the wind-shear signal vector, $\boldsymbol{x}_{\mathrm{c}}$ denotes the clutter signal vector, and $\boldsymbol{x}_{\mathrm{n}}$ is the thermal noise vector with a Gaussian distribution.

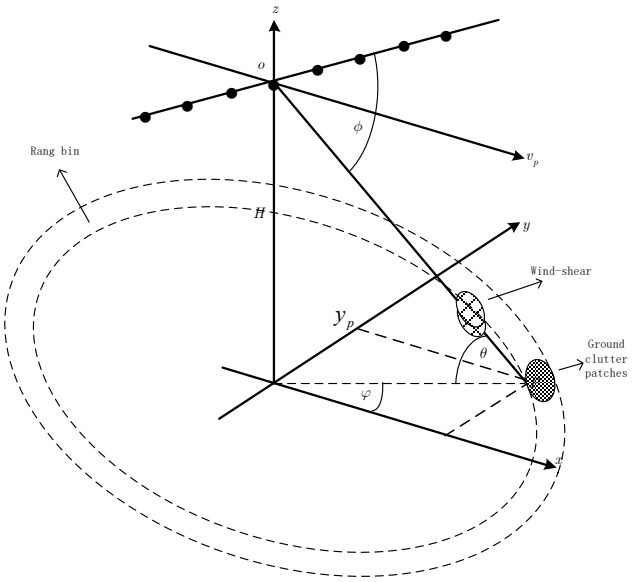

Fig. 2. The geometry of the forward-looking array weather radar.

2.1 Signal of Wind-Shear

The signal of the wind-shear received by M antenna elements and sampled by N pulses, then an NM-dimensional measurement vector of wind-shear $\boldsymbol{x}_\mathrm{s}$ can be obtained. Due to the power of the wind-shear is much lower than that of clutter, only the main lobe signal of wind-shear is considered. $\boldsymbol{x}_\mathrm{s}$ in the lth range bin can be expressed as:

$$\boldsymbol{x}_\mathrm{s}^{(l)} = b_\mathrm{s}\boldsymbol{s}(f_\mathrm{d}, f_\mathrm{s}) \tag{2}$$

where b_s is complex amplitude of the wind-shear. $\boldsymbol{s}(f_\mathrm{d}, f_\mathrm{s})$ is the NM-dimensional space-time steering vector with the Doppler frequency f_d and the spatial frequency f_s, i.e., $\boldsymbol{s}(f_\mathrm{d}, f_\mathrm{s}) = \boldsymbol{s}_\mathrm{d}(f_\mathrm{d}) \otimes \boldsymbol{s}_\mathrm{s}(f_\mathrm{s})$, which can be expressed as:

$$\boldsymbol{s}_\mathrm{d}(f_\mathrm{d}) = [1 \quad \exp(\mathrm{j}f_\mathrm{d}) \quad \cdots \quad \exp(\mathrm{j}(N-1)f_\mathrm{d})]^\mathrm{T}, \tag{3}$$

$$\boldsymbol{s}_\mathrm{s}(f_\mathrm{s}) = [1 \quad \exp(\mathrm{j}f_\mathrm{s}) \quad \cdots \quad \exp(\mathrm{j}(M-1)f_\mathrm{s})]^\mathrm{T} \tag{4}$$

where

$$f_\mathrm{d} = \frac{4\pi v_l}{\lambda f_\mathrm{r}}, \tag{5}$$

$$f_\mathrm{s} = \frac{2\pi d}{\lambda}\cos\theta\cos\varphi = \frac{2\pi d}{\lambda}\cos\phi \tag{6}$$

where θ and φ are the azimuth and pitch angle of the wind-shear respectively, ϕ is the spatial cone angle. v_l is statistical average of the radial velocity of all the meteorological particles in the lth range bin, namely the wind speed.

2.2 Signal of Ground Clutter

As shown in Fig. 2, the clutter in a range ring can be model as a superposition of signals from N_c independent clutter patches distributed in the azimuth direction, which can be expressed as:

$$\boldsymbol{x}_\mathrm{c}^{(l)} = \sum_{i=1}^{N_\mathrm{c}} a_i \boldsymbol{s}(f_{\mathrm{d},i}, f_{\mathrm{s},i}) \tag{7}$$

where

$$f_{\mathrm{d},i} = \frac{2v_\mathrm{p}}{\lambda f_\mathrm{r}}\cos\varphi_i\cos\theta_i, \tag{8}$$

$$f_{\mathrm{s},i} = \frac{d}{\lambda}\cos\phi = \cos(\varphi_i - \psi). \tag{9}$$

3. Wind Speed Estimation and Off-grid Problem

3.1 Wind Speed Estimation Based on On-grid Sparse Recovery

The received signal of the wind-shear is mixed with the signal of ground clutter, before we estimate the wind speed, the clutter should be suppressed firstly. The space-time adaptive processing (STAP) is an effective method for clutter suppression [9], [10]. The linear transformation can be designed based on space-time interpolation, then the clutter-and-noise covariance matrix is obtained, and after clutter suppression the wind-shear observation with the wind speed to be estimated can be expressed as:

$$\overline{\boldsymbol{x}}^{(l)} = \boldsymbol{x}_\mathrm{s}^{(l)} + \boldsymbol{x}_\mathrm{n}^{(l)}. \tag{10}$$

The wind-shear is consisted by a large number of metrological particles, and the wind speed of the range bin is the statistical average of the velocity of all the particles in the range bin. The Doppler frequency is related to the wind speed, as shown in (5) and it is considered to be sparse in the frequency domain. The redundant dictionary is constructed by space-time steering vectors with different Doppler frequency (related to the wind speed), then the wind speed estimation is transformed to the sparse recovery problem.

$$\overline{\boldsymbol{x}}^{(l)} = \boldsymbol{\Psi}\boldsymbol{\alpha} + \boldsymbol{n}, \tag{11}$$

where $\boldsymbol{\Psi}$ denotes the redundant space-time steering dictionary, $\boldsymbol{\alpha} = [a_1, \ldots, a_{N_\mathrm{d}}]^\mathrm{T} \in \mathbb{R}^{N_\mathrm{d}\times 1}$ is an unknown solution vector, where each row represents a possible wind speed. When the radar scans the wind-shear in a certain orientation ϕ, the f_s is a constant. The wind speed v_l is related to f_d, according to the range of the wind speed, the wind speed domain is discretized into N_d grid points, e.g., $v_l \in \{V\} = \{v_l^{(1)}, \ldots, v_l^{(N_\mathrm{d})}\}$. The corresponding set of the space-time steering vectors of all grid points can be formulated as:

$$\boldsymbol{\Psi} = \boldsymbol{S}_\mathrm{d} \otimes \boldsymbol{S}_\mathrm{s} = [\boldsymbol{\psi}_1, \boldsymbol{\psi}_2, \ldots, \boldsymbol{\psi}_{N_\mathrm{d}}] \in \mathbb{C}^{NM\times N_\mathrm{d}} \tag{12}$$

where

$$\boldsymbol{S}_{\mathrm{d}}=\begin{bmatrix} 1 & 1 & \cdots & 1 \\ \exp\left(\mathrm{j}\dfrac{4\pi v_l^{(1)}}{\lambda f_{\mathrm{r}}}\right) & \exp\left(\mathrm{j}\dfrac{4\pi v_l^{(2)}}{\lambda f_{\mathrm{r}}}\right) & \cdots & \exp\left(\mathrm{j}\dfrac{4\pi v_l^{(N_{\mathrm{d}})}}{\lambda f_{\mathrm{r}}}\right) \\ \vdots & \vdots & \cdots & \vdots \\ \exp\left(\mathrm{j}(N-1)\dfrac{4\pi v_l^{(1)}}{\lambda f_{\mathrm{r}}}\right) & \exp\left(\mathrm{j}(N-1)\dfrac{4\pi v_l^{(2)}}{\lambda f_{\mathrm{r}}}\right) & \cdots & \exp\left(\mathrm{j}(N-1)\dfrac{4\pi v_l^{(N_{\mathrm{d}})}}{\lambda f_{\mathrm{r}}}\right) \end{bmatrix}, \tag{13}$$

$$\boldsymbol{S}_{\mathrm{s}}=\begin{bmatrix} 1 \\ \exp\left(\mathrm{j}\dfrac{2\pi d}{\lambda}\cos\theta\cos\varphi\right) \\ \vdots \\ \exp\left(\mathrm{j}(M-1)\dfrac{2\pi d}{\lambda}\cos\theta\cos\varphi\right) \end{bmatrix}. \tag{14}$$

According to the theory of sparse recovery, the solution vector $\boldsymbol{\alpha}$ can be the method such as orthogonal match pursuit.

3.2 Off-grid Problem

Although the sparse recovery methods can obtain good performance with only limited number of pulse samples, the wind speed is not always located in the discretized grid points in the wind speed domain $\{V\}$, and the off-grid effect can degrade the performance of wind speed estimation significantly.

To solve the off-grid problem, a theory of super-resolution for frequency estimation has been recently introduced [16], and a gridless convex optimization method known as atomic norm minimization was proposed [17].

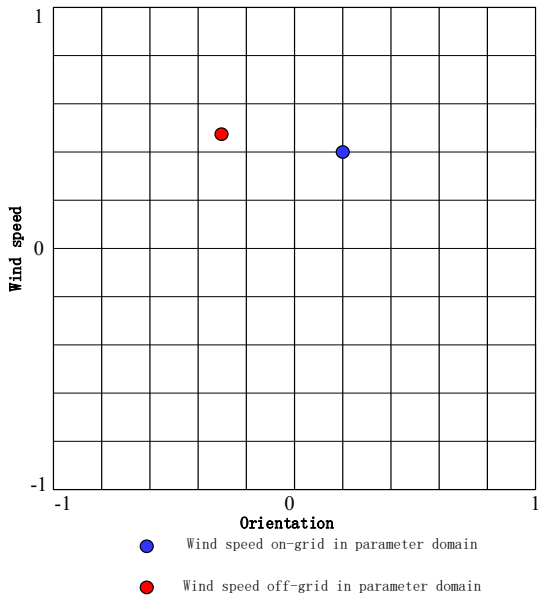

Fig. 3. The off-grid problem of wind speed estimation.

4. Gridless Sparse Recovery-based Wind Speed Estimation with Multiple Measurements

A gridless sparse recovery-based wind speed estimator with multiple measurement vectors is suggested to address the off-grid issue and enhance wind speed estimate performance.

The above-mentioned sparse recovery-based wind speed estimation method only utilize a single measurement vector for sparse recovery, while joint sparse recovery of multiple measurement vectors can significantly improve the performance of wind speed sparse recovery [14]. Each element of the airborne array radar undergoes pulse sampling to obtain multi-channel spatial sampling data. Therefore, after clutter suppression with STAP, this paper uses phase compensation for multi-channel spatial sampling data to construct multiple Doppler measurement vectors for wind speed estimation.

There is a relationship between the first array element and the data received by the mth array element as shown in (15)

$$\bar{\boldsymbol{x}}^{(1)}=\bar{\boldsymbol{x}}^{(m)}\odot\left[\mathrm{e}^{-\mathrm{j}m\phi}\quad \mathrm{e}^{-\mathrm{j}m\phi}\quad \ldots\quad \mathrm{e}^{-\mathrm{j}m\phi}\right]^{\mathrm{T}}_{(N\times 1)}, \tag{15}$$

where $\odot$ denotes the Hadamard product, and ϕ is the spatial cone angle of radar beam direction.

Using the first array element as the reference array element, then we use (15) for spatial phase compensation of other array elements, M Doppler frequency measurement vectors $\bar{\boldsymbol{X}}=[\bar{\boldsymbol{x}}^{(1)},\bar{\boldsymbol{x}}^{(2)},\ldots,\bar{\boldsymbol{x}}^{(M)}]$ can be obtained. The schematic diagram of spatiotemporal sampling before and after phase compensation is shown in Fig. 4.

The measurements of wind-shear can be tensored by the space-time steering vectors, and the covariance matrix of the wind-shear measurements $\bar{\boldsymbol{X}}$ can be decomposed in the following form:

$$\boldsymbol{R}=\sum_{i=1}E\left\{\left|\gamma_i\right|^2\right\}\boldsymbol{s}(f_d,f_s)\boldsymbol{s}(f_d,f_s)^{\mathrm{H}}+{\sigma_{\mathrm{n}}}^2\boldsymbol{I}_{MN}, \tag{16}$$

where $\boldsymbol{R}$ is a semi-positive definite Hermitian matrix with block Toeplitz structure and low-rank features, σ_{n}^2 is the noise power, and $\boldsymbol{I}_{\mathrm{MN}}$ is the unit matrix with $NM\times NM$ dimension.

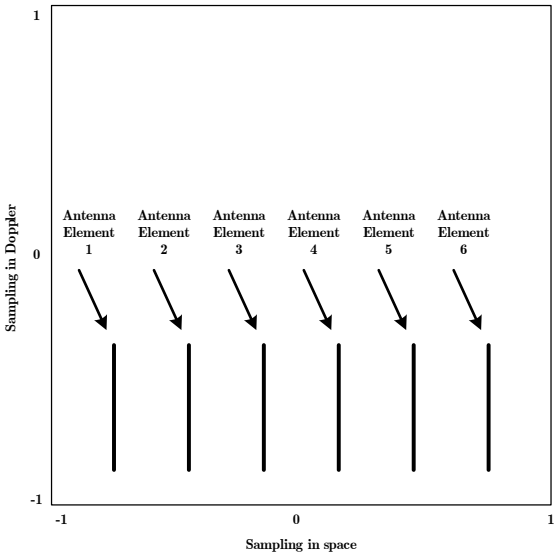

(a) Before spatial phase compensation

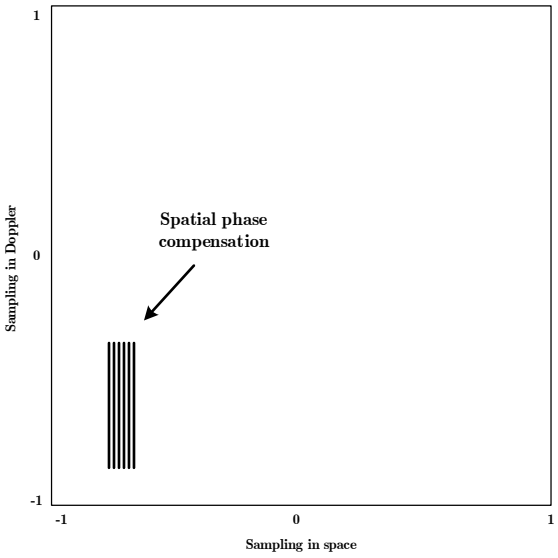

(b)After spatial phase compensation

Fig. 4. Spatial phase compensation.

The set of space-time steering vectors in the continuous wind speed domain can be regarded as an atomic set $\mathcal{A}$ and defined as:

$$\mathcal{A} \triangleq \left\{ \boldsymbol{s}(f_{\mathrm{d}}, f_{\mathrm{s}}) = \boldsymbol{s}_{\mathrm{d}}(f_{\mathrm{d}}) \otimes \boldsymbol{s}_{\mathrm{s}}(f_{\mathrm{s}}) \,|\, f_{\mathrm{d}} \in (-1,1), f_{\mathrm{s}} = \frac{2\pi d}{\lambda} \cos\phi \right\}. \tag{17}$$

According to the low-rank matrix recovery theory and the sparse properties of clutter, the sparse recovery of $\bar{\boldsymbol{X}}$ in the continuous null time plane can be expressed in the form of the following mixed norm, known as the atomic norm.

$$\left\| \bar{\boldsymbol{X}} \right\|_{\mathcal{A}} \triangleq \inf_{f_{\mathrm{d}}, f_{\mathrm{s}}, \boldsymbol{a}_k} \left\{ \sum_k \left\| \boldsymbol{a}_k \right\|_2 : \bar{\boldsymbol{X}} = \sum_k \boldsymbol{a}_k \boldsymbol{s}(f_{\mathrm{d},k}, f_{\mathrm{s}}) \right\}. \tag{18}$$

The wind-shear measurements $\bar{\boldsymbol{X}}$ and the subspace $\boldsymbol{S}(\boldsymbol{T})$ can be obtained from the above atomic norm minimization.

$$\bar{\boldsymbol{X}}_{\mathrm{s}} = \arg\min_{\bar{\boldsymbol{X}}_{\mathrm{s}}} \quad \left\| \bar{\boldsymbol{X}}_{\mathrm{s}} \right\|_{\mathcal{A}}, \quad \text{s.t. } \left\| \bar{\boldsymbol{X}}_{\mathrm{s}} - \bar{\boldsymbol{X}} \right\|_{\mathrm{F}}^2 \le K\varepsilon. \tag{19}$$

The following semi-positive definite planning issue may be created from the atomic norm minimization in (19).

$$\begin{aligned} &\left\{ \boldsymbol{X}_{\mathrm{c}}, \boldsymbol{S}(\boldsymbol{T}) \right\} = \arg\min_{\boldsymbol{u}, \boldsymbol{X}_{\mathrm{c}}} \quad \frac{1}{2\sqrt{NM}} \left[\mathrm{tr}\, \boldsymbol{S}(\boldsymbol{T}) + \mathrm{tr}(\boldsymbol{\Phi}) \right], \\ &\text{s.t. } \begin{bmatrix} \boldsymbol{\Phi} & \boldsymbol{X}^{\mathrm{H}} \\ \boldsymbol{X} & \boldsymbol{S}(\boldsymbol{T}) \end{bmatrix} \ge 0, \boldsymbol{\Phi} = \boldsymbol{\Phi}^{\mathrm{H}}, \left\| \boldsymbol{X}_{\mathrm{c}} - \boldsymbol{X} \right\|_{\mathrm{F}}^2 \le K\varepsilon \end{aligned} \tag{20}$$

where $\boldsymbol{\Phi}$ is a $M \times M$ dimensional Hermitian matrix, $\boldsymbol{S}(\boldsymbol{T})$ is a is a $N \times N$ dimensional Block Toeplitz matrix.

The obtained subspace $\boldsymbol{S}(\boldsymbol{T})$ of the wind-shear is subjected to a block Toeplitz matrix decomposition, and the normalized Doppler frequency f_{d} can be estimated. Then the wind speed v_l can be calculated by (5).

The algorithm of gridless sparse recovery-based wind speed estimation is given in Algorithm 1.

Algorithm 1. Gridless sparse recovery-based wind speed estimation

Step 1: Signal of radar in the lth (l = 1,2,…,L) range bin $\boldsymbol{x}^{(l)}$ is received.

Step 2: The ground clutter can be suppressed by STAP, then the wind-shear observation can be expressed as $\bar{\boldsymbol{x}}^{(l)}$.

Step 3: Spatial phase compensation of array elements, M Doppler frequency measurement vectors $\bar{\boldsymbol{X}} = [\bar{\boldsymbol{x}}^{(1)}, \bar{\boldsymbol{x}}^{(2)}, \ldots, \bar{\boldsymbol{x}}^{(M)}]$ can be obtained by (15).

Step 4: The wind-shear measurements $\bar{\boldsymbol{X}}$ and the subspace $\boldsymbol{S}(\boldsymbol{T})$ can be obtained from the atomic norm minimization by (20).

Step 5: The normalized Doppler frequency f_{d} can be estimated from $\boldsymbol{S}(\boldsymbol{T})$ by a block Toeplitz matrix decomposition.

Step 6: The wind speed v_l can be calculated by (5).

5. Numerical Results

In this section, we demonstrate and compare the performance of the proposed wind speed estimation method to the conventional methods using simulated data. The simulated wind field data of wind-shear is generated by the computational fluid dynamic (CFD) software Ansys Fluent [18], the wind-shear is in 8.5 km–16.5 km ahead of the aircraft. The signal of wind-shear is received by the airborne array weather radar, which has M = 8 elements, and inter-element spacing is half wavelength ($d = \lambda/2$). The parameters in our simulations are set as follows: PRF = 7000 Hz, wavelength λ = 0.05 m, platform height H = 600 m. The platform velocity v_{p} = 75 m/s. Signal to noise rate of the wind-shear SNR = 5 dB. Clutter to noise rate CNR = 40 dB.

The proposed method is compared with the existing wind speed algorithms, such as pulse pair processing method [12], fast Fourier transform method [13] and on-grid sparse recovery-based wind speed method [14]. In the

on-grid CS method, we set the wind speed to a range of –60 m/s to 60 m/s, a dictionary is built according to (12) with intervals set to 0.5 m/s.

Figure 5 shows the performance of the four estimate methods for wind speed estimation. We can see that when the number of pulses is more sufficient ($N = 64$), the PPP method and the FFT are also able to estimate the wind shear wind speed more effectively, as shown in Fig. 5(a). However, when the number of pulses is insufficient ($N = 32$), the wind speed estimation performance of PPP method and FFT method decreases obviously, as shown in Fig. 5(b). On-grid CS method and the proposed method can estimate the wind speed efficiently when the number of pulses is sufficient and insufficient. But the wind speed estimation result of the proposed method solves the real value of the wind speed more accurate, because the wind shear wind speed is changing continuously, and the wind speed estimation obtained by the on-grid CS method is not as efficient as that obtained by the proposed method due to the continuous change of wind speed. The wind speed estimates obtained by the on-grid CS method can only obtain sparse support peaks at the neighboring dictionary grid points due to the dictionary mismatch, and they are two peaks, which leads to the estimation error, as shown in Fig. 6. In this paper, since the method is gridless sparse recovery in continuous parameter space, the method in this paper produces a peak at the true value of the target speed parameter and can estimate the wind speed parameter more accurately.

Table 1 shows the running time comparison. We can see that the running time increases rapidly when the dictionary interval decreases from 2 m/s to 0.5 m/s, and even the interval is set to 0.5 m/s the performance of the on-grid method is worse than the proposed method, but the running time is about 8 times of the proposed method. Although, the running time of the PPP method and FFT method is less than the proposed method, we can see that these two methods cannot estimate the wind speed accurately when the number of pulses is insufficient.

Figure 7 shows the comparison of the estimation results between the proposed method and the on-grid CS method with different dictionary intervals. The sparse recovery dictionaries with intervals 0.5 m/s, 1 m/s and 2 m/s in the range of –60 m/s to 60 m/s are constructed for the on-grid CS method, respectively, i.e., the larger the dictionary intervals are, the more serious is the problem of dictionary mismatch. The performance of the on-grid CS method decreases significantly as the dictionary interval increases (from 0.5 m/s to 2 m/s), which indicates that the estimation performance of the method mainly depends on

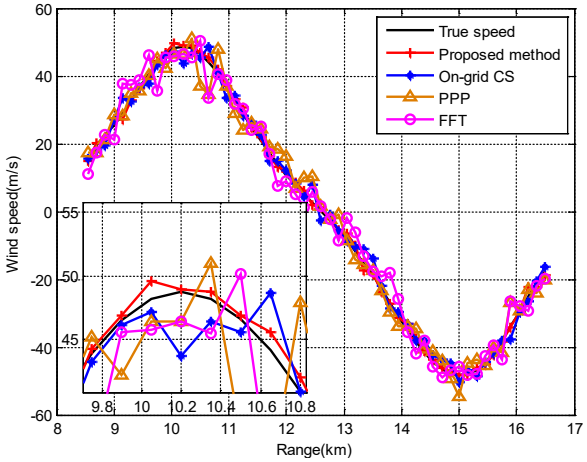

(a) $N = 64$

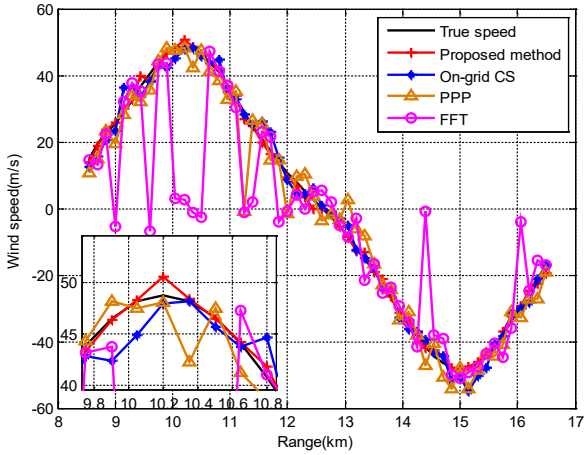

(b) $N = 32$

Fig. 5. Wind speed estimates with different number of pulses.

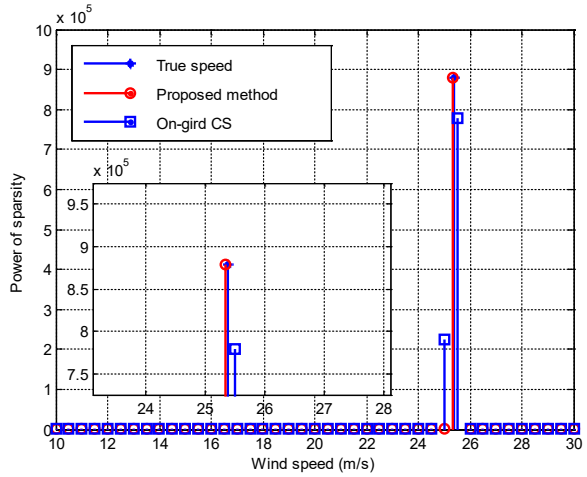

Fig. 6. Wind speed estimates in the case of dictionary mismatch.

Method	Proposed method	On-grid method (0.5 m/s)	On-grid method (1.0 m/s)	On-Grid method (2.0 m/s)	PPP method	FFP method
Running time (s)	0.1512	1.1675	0.4875	0.2127	0.0937	0.1135

Tab. 1. Running time comparison.

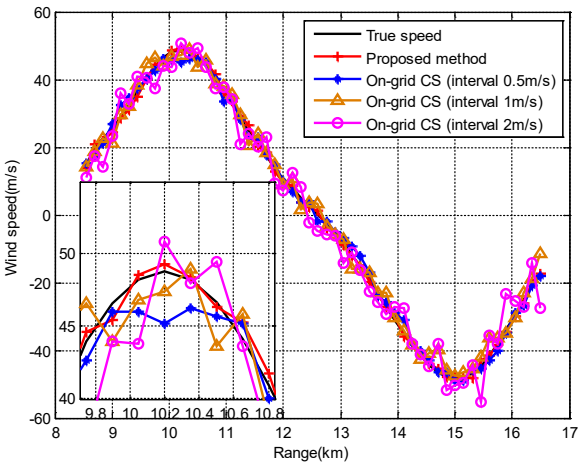

Fig. 7. Wind speed estimates with different dictionary intervals.

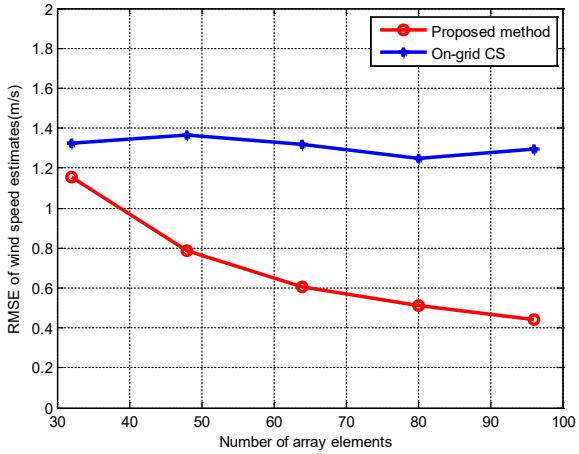

Fig. 8. Wind speed estimates with different number of array elements.

the dictionary interval. When the wind speed parameters do not fall on the pre-set dictionary grids, the estimation performance of the method decreases significantly due to the dictionary mismatch. On the other hand, the wind speed estimation performance of the proposed method is better than that of the on-grid CS method due to the sparse recovery on the continuous wind speed domain.

Figure 8 shows the RMSE of wind speed estimation with the number of array elements. When the number of array elements increases, the wind speed estimation performance of the proposed method is obviously improved, which is due to the construction of multiple measurement vectors by the multi-channel data spatial phase compensation. Multiple observation vectors can obviously improve the performance of the sparse recovery and improve the accuracy of wind speed estimation. On the other hand, the on-grid CS method does not construct multi-observation vector sparse recovery, so the increase of the number of array elements has little effect on the estimation performance.

6. Conclusion

The dictionary mismatch degrades the performance of wind speed estimation significantly. This paper proposed a gridless sparse recovery-based method for wind speed estimation based on atomic norm minimization. Joint sparse recovery measurements are constructed by compensated spatial samples with wind-shear orientation information. The proposed method can effectively improve the accuracy of wind speed estimation under dictionary mismatch, and the estimation performance is better than that of the existing sparse recovery-based method of wind speed estimation with the pre-set discretized dictionary.

Acknowledgments

This work was supported by the National Key Research and Development Program of China (2022YFB3904304).

References

[1] LUCCHI, G. A new airborne weather radar systems. *Journal of Aircraft*, 2015, vol. 19, no. 3, p. 239–245. DOI: 10.2514/6.1981-237

[2] BAXA, E. G. Airborne pulsed Doppler radar detection of low-altitude windshear – A signal processing problem. *Digital Signal Processing*, 1991, vol. 1, no. 4, p. 186–197. DOI: 10.1016/1051-2004(91)90112-X

[3] LIN, C., ZHANG, K., CHEN, X., et al. Overview of low-level wind shear characteristics over Chinese mainland. *Atmosphere*, 2021, vol. 12, no. 5, p. 1–19. DOI: 10.3390/atmos12050628

[4] BRACALENTE, M., BRITT, L., JONES, R. Airborne Doppler radar detection of low altitude windshear. *Journal of Aircraft*, 1990, vol. 27, no. 2, p. 151–157. DOI: 10.2514/3.45911

[5] BAXA, E. G., LAI, Y. C., KUNKEL, M. W. New signal processing developments in the detection of low-altitude windshear with airborne Doppler radar. *The Record of the 1993 IEEE National Radar Conference*. Lynnfield (USA), 1993, p. 269 to 274. DOI: 10.1109/NRC.1993.270452

[6] RTCA. *Minimum Operational Performance Standards (MOPS) for Airborne Weather Radar with Forward-Looking Windshear and Turbulent Detection Capability*. 212 pages. [Online] Cited 2018-08-17. Available at: https://products.rtca.org/21dimut/

[7] BAXA, E. G., DESHPANDE, M. D. *Signal Processing Techniques for Clutter Filtering and Wind Shear Detection (NASA Report)*. 44 pages. [Online] Cited 2013-09-06. Available at: https://ntrs.nasa.gov/citations/19910014841

[8] KLEMM, R. *Principle of Space-time Adaptive Processing*. 3rd ed. London (UK): IET Publishers, 2006. ISBN: 9780863415661

[9] ZHANG, Y., WANG, S. Remote relative wind velocity estimation using airborne Doppler radar and spectrum analysis. *IEEE Transactions on Aerospace and Electronic Systems*, 2001, vol. 47, no. 3, p. 1648–1667. DOI: 10.1109/TAES.2011.5937256

[10] LI, H., CHEN, Y., FENG, K., et al. Low-altitude windshear wind speed estimation method based on KASPICE-STAP. *Sensors,* 2023, vol. 23, no. 54, p. 1–17. DOI: 10.3390/s23010054

[11] OSEGUERA, R. M., BOWLES, R. L., ROBINSON, P. A. Airborne in situ computation of the wind shear hazard index. *AIAA Journal*, 1992. DOI: 10.2514/6.1992-291

[12] BAXA, E. G., LEE, J. The pulse-pair algorithm as a robust estimator of turbulent weather spectral parameters using airborne pulse Doppler radar. (NASA Report) 42 pages. [Online] Cited 2013-09-06. Available at: https://ntrs.nasa.gov/citations/19910018088

[13] BRITT, C., HARRAH, T., GRITTENDEN, L. Microburst hazard detection performance of the NASA experimental windshear radar system. In *Aircraft Design, Systems, and Operations Meeting*. Monterey (USA), 1993. DOI: 10.2514/6.1993-3943

[14] LI, H., ZHOU, M., GUO, Q., et al. Compressive sensing-based wind speed estimation for low-altitude wind-shear with airborne phased array radar. *Multidimensional Systems and Signal Processing*, 2018, vol. 29, no. 2, p. 719–732. DOI: 10.1007/s11045-016-0448-6

[15] CANDES, E. J., WAKIN, M. B. An introduction to compressive sampling. *IEEE Signal Processing Magazine*, 2008, vol. 25, no. 2, p. 21–30. DOI: 10.1109/MSP.2007.914731

[16] TANG, G., BHASKAR, B., SHAH, P., et al. Compressed sensing off the grid. *IEEE Transactions on Information Theory*, 2013, vol. 59, no. 11, p. 7465–7490. DOI: 10.1109/TIT.2013.2277451

[17] CANDES, E. J., FERNANDEZ-GRANDA, C. Towards a mathematical theory of super-resolution. *Communications on Pure and Applied Mathematics*, 2014, vol. 67, no. 6, p. 906–956. DOI: 10.1002/cpa.21455

[18] FAN, Y., WU, R., MENG, Z., et al. Wind shear signal simulation of the airborne weather radar. In *Proceedings of the 2011 IEEE Radar Conference*. Kansas City (USA), 2011, p. 710–713. DOI: 10.1109/RADAR.2011.5960630

About the Authors …

Zhiming ZHENG was born in Fujian, China. He received his M.Sc. from Nanjing University of Aeronautics and Astronautics in 2010. Now he is a Ph.D. candidate in Nanjing University of Aeronautics and Astronautics. His research interests include airborne weather radar, array signal processing.